

Theoretical studies of low-energy electron-CO₂ scattering: Total, elastic, and differential cross sections

T. N. Rescigno,¹ D. A. Byrum,² W. A. Isaacs,³ and C. W. McCurdy³

¹*Physics and Space Technology Directorate, Lawrence Livermore National Laboratory, Livermore, California 94551*

²*Department of Applied Science, University of California–Davis, Livermore, California 94551*

³*Computing Sciences Directorate, Lawrence Berkeley National Laboratory, Berkeley, California 94720*

(Received 9 March 1999)

We report the results of a theoretical study of electron scattering by CO₂ at incident electron energies ranging from 0.25 to 10 eV using the complex Kohn variational method. These are the first fully *ab initio* calculations to accurately reproduce the two dominant features observed in experiment, namely, the dramatic rise in the integral cross sections below 2.0 eV and the resonance enhancement near 3.8 eV. Both of these effects are sensitive to the inclusion of electronic correlation effects involving long-range target polarization and short-range distortion. We have also carried out a preliminary study of effects of target vibrational motion in ²Π_u symmetry with an adiabatic nuclei treatment of the symmetric stretch mode. We find that this has a substantial effect on the width of the 3.8 eV resonance feature and gives results for both the integral elastic and total cross sections in excellent agreement with experiment. Our calculated differential elastic cross sections are also in good accord with recent experimental results. [S1050-2947(99)09409-3]

PACS number(s): 34.80.Bm

I. INTRODUCTION

Carbon dioxide (CO₂) is an important atmospheric constituent and plays a key role in many gaseous electronics applications. Electron collision processes involving CO₂ are of fundamental and practical importance; in addition, there are several features in the low-energy cross sections that pose some challenging theoretical questions. For these reasons, electron-CO₂ scattering continues to attract the attention of both experimentalists and theorists. Since the pioneering work of Morrison, Lane, and Collins [1], who performed the first close-coupling calculations on this system using model potentials, interest has continued to focus on the two prominent features that dominate the low-energy integral cross sections, namely, the dramatic rise in the cross sections below 2.0 eV and the resonance peak centered near 3.8 eV. Theoretical studies have established that the resonance behavior arises from the presence of a short-lived ²Π_u negative-ion state and that the low-energy behavior is consistent with the presence of a virtual state. This interpretation of the low-energy behavior was first suggested by Morrison [2], but being based on conclusions drawn from model potential calculations, it had been regarded with skepticism on the part of some investigators [3]. There have been several other model potential calculations, carried out with varying degrees of sophistication, but they have not been able to reproduce the low-energy (<2 eV) behavior observed in the integral cross sections. Most previous *ab initio* calculations have been carried out at the static-exchange level and hence cannot describe any low-energy feature that is sensitive to target polarization effects. The recent *R*-matrix study of Morgan [4] is the first calculation of *e*-CO₂ scattering to treat electron-target correlation in a completely *ab initio* fashion and to verify that the low-energy rise in the cross section is caused by a virtual state.

While previous theoretical studies have illuminated many

aspects of *e*-CO₂ scattering, none have achieved more than qualitative agreement with experiment below 8 eV. With the recent publication of two new experimental cross beam studies of elastic *e*-CO₂ scattering [5,6], we now have absolute differential cross sections over a broad energy range. These studies have served to spotlight the inability of any previous theoretical calculation to achieve even qualitatively correct differential cross sections at collision energies below 5 eV. The present study was undertaken to address the need for calculations on this system that reflect the level of sophistication that can be achieved with modern *ab initio* methods and to try to remedy “the poor level of agreement which exists between theory and experiment at energies below about 6 eV” [6].

II. COMPLEX KOHN VARIATIONAL METHOD

The complex Kohn method is a variational technique which imposes outgoing-wave boundary conditions through the use of a trial wave function built from both square-integrable (Cartesian Gaussian) and continuum basis functions. Since detailed descriptions of the method have been given elsewhere [7,8], we will limit ourselves here to a summary of its salient features. This work was restricted to electronically elastic scattering; consequently, we used a trial wave function of the form

$$\Psi_r = A[\chi_0(r_1 \cdots r_N)F_0(r_{N+1})] + \sum_i d_i \Theta_i(r_1 \cdots r_{N+1}), \quad (1)$$

where χ_0 is the ground-state target wave function, F_0 is the function that describes the scattered electron, and A is the antisymmetrization operator. The functions $\{\Theta_i\}$ are a set of $(N+1)$ -electron, antisymmetrized configuration-state functions (CSFs) that are used to describe polarization and/or

correlation effects due to (electronically) closed channels. In the Kohn method, the single-particle function F_0 is further expanded as

$$F_0(\mathbf{r}) = \sum_{lm} [f_l(r) \delta_{l0} \delta_{mm_0} + T_{lm_0m_0} g_l(r)] Y_{lm}(\hat{\mathbf{r}})/r + \sum_k c_k \phi_k(\mathbf{r}) \quad (2)$$

in a basis of symmetry-adapted molecular orbitals, $\phi_k(\mathbf{r})$, along with products of spherical harmonics, $Y_{lm}(\hat{\mathbf{r}})$, and regular (Riccati–Bessel) and outgoing continuum functions, $f_l(r)$ and $g_l(r)$, respectively. The partial-wave T -matrix elements, $T_{lm_0m_0}$ are the fundamental dynamical quantities from which all cross sections are derived. These are obtained by solving the set of complex linear equations [7] that derive from making the Kohn functional

$$T^s(c, d, T) = T - 2 \int \Psi_r (H - E) \Psi_r \quad (3)$$

stationary with respect to variations in the quantities c, d , and T defined in Eqs. (1) and (2).

The function given in Eq. (1) is quite general and can, in principle, be used to carry out calculations with elaborate trial wave functions of arbitrary complexity. In the present study, we approximated the electronic target state as the Hartree-Fock wave function for the ground state of CO_2 . Consistent with this choice, we restricted the $(N+1)$ -electron CSFs $\{\Theta_i\}$ to those constructed as products of bound molecular orbitals and terms obtained by singly exciting the target Hartree-Fock wave function. We used different prescriptions to build this correlation portion of the trial wave function, depending on the symmetry under consideration. These prescriptions will be described further below.

III. ADIABATIC NUCLEI APPROXIMATION AND VIBRATIONAL MOTION

The preponderance of electron-molecule calculations that have been reported in the existing literature were performed with the target nuclei fixed at their equilibrium positions. The cross sections so calculated correspond, in general, to rotationally and vibrationally summed quantities in cases where the internal motion of the target nuclei can be ignored. Because this approximation breaks down for CO_2 in the resonance region, it is useful to recall the arguments used to justify the fixed-nuclei result. For *nonpolar* targets, when the incident electron energy is large with respect to the rotational energy spacings of the molecule, one is usually justified in ignoring the rotational motion of the target and treating the scattering as that produced by a collection of randomly oriented, motionless targets [9]. Under this assumption, the differential cross section (DCS) for exciting a molecule from initial vibrational state v to final vibrational state v' is given by an average over orientations of the molecule:

$$\frac{d\sigma}{d\theta}(v \rightarrow v') = \frac{4\pi}{k_v^2} \int \frac{d\alpha d\beta d\gamma}{8\pi^2} |\langle k_{v'} v' | \mathbf{T} | k_v v \rangle|^2, \quad (4)$$

where α, β , and γ are the three Euler angles that orient the initial and final wave vectors \mathbf{k}_v and $\mathbf{k}_{v'}$ with respect to the target and the laboratory scattering angle Θ is the angle between \mathbf{k}_v and $\mathbf{k}_{v'}$. We make the Born-Oppenheimer approximation for the scattering states and write them as products of electronic continuum functions times target vibrational functions. Furthermore, if we ignore the dependence of the free-electron wave vector on the target vibrational state, then the body-frame T matrix has the expansion

$$\langle k_{v'} v' | \mathbf{T} | k_v v \rangle \approx \sum_{l'l'm'm'} i^{l-l'} Y_{lm}(\hat{\mathbf{k}}) Y_{l'm'}^*(\hat{\mathbf{k}}) \times \int \eta_{v'}(\mathbf{s}) T_{lm'l'm'}(\mathbf{s}) \eta_v(\mathbf{s}) d\mathbf{s}, \quad (5)$$

where the vibrational wave functions are η_v and $\eta_{v'}$ and we have used \mathbf{s} to denote the internal vibrational coordinates of the target. Thus the adiabatic nuclei approximation for vibrational excitation cross sections [10] requires integrals of the individual fixed-nuclei T -matrix elements, which depend parametrically on internal target geometry, between the target vibrational wave functions. If we are not interested in the excitation of individual vibrational levels, then we can sum Eq. (4) over the final v' , using the closure relation

$$\sum_{v'} \eta_{v'}(\mathbf{s}) \eta_{v'}(\mathbf{s}') = \delta(\mathbf{s} - \mathbf{s}') \quad (6)$$

to obtain

$$\frac{d\sigma^{\text{total}}}{d\theta} = \int \eta_v(\mathbf{s})^2 \frac{d\sigma}{d\theta}(\mathbf{s}) d\mathbf{s}. \quad (7)$$

Thus the vibrationally summed cross section is expressed as the expectation value of the fixed-nuclei cross section over the initial target vibrational state. If we make the further approximation that the fixed-nuclei cross section is independent of nuclear geometry in the Franck-Condon region of the ground state, then the quantity $d\sigma/d\theta|_{\mathbf{s}=\mathbf{s}_0}$ can be taken outside the integral in Eq. (7), leading to the approximation most frequently encountered in the literature. We shall find that this latter approximation is not valid in the present case.

IV. CALCULATIONS

In all our calculations, we employed a self-consistent field (SCF), Hartree-Fock target wave function for the ground state of CO_2 using a $(9s\ 5p\ 1d)$ basis of Cartesian Gaussian functions, contracted to $[5s\ 3p\ 1d]$ [11]. To construct the Kohn trial function, the target basis was augmented with the additional Gaussian functions listed in Table I. To complete the expansion of the trial scattering function, we included numerically generated continuum basis functions, retaining terms with angular momentum quantum numbers l and $|m|$ less than or equal to 6. Although we will use irreducible representation designations appropriate to the point group

TABLE I. Gaussian basis sets used in e -CO₂ scattering calculations.

| Center | Type | Exponent | Coefficient ^a | Center | Type | Exponent | Coefficient ^a |
|--------------|----------|----------|--------------------------|---|----------|----------|--------------------------|
| Target basis | | | | Supplemental scattering basis, Σ_g , Σ_u , and Π_u symmetries | | | |
| Carbon | <i>s</i> | 4232.61 | 0.006228 | Carbon | <i>s</i> | 0.0613 | 1.000000 |
| Carbon | <i>s</i> | 634.882 | 0.047676 | Carbon | <i>s</i> | 0.0245 | 1.000000 |
| Carbon | <i>s</i> | 146.097 | 0.231439 | Carbon | <i>s</i> | 0.0098 | 1.000000 |
| Carbon | <i>s</i> | 42.4974 | 0.789108 | Carbon | <i>p</i> | 0.0441 | 1.000000 |
| Carbon | <i>s</i> | 14.1892 | <u>0.791751</u> | Carbon | <i>p</i> | 0.017 | 1.000000 |
| Carbon | <i>s</i> | 1.96660 | 0.321870 | Carbon | <i>p</i> | 0.0065 | 1.000000 |
| Carbon | <i>s</i> | 5.14770 | <u>1.000000</u> | Oxygen | <i>s</i> | 0.1138 | 1.000000 |
| Carbon | <i>s</i> | 0.49620 | 1.000000 | Oxygen | <i>s</i> | 0.0455 | 1.000000 |
| Carbon | <i>s</i> | 0.15330 | 1.000000 | Oxygen | <i>s</i> | 0.0182 | 1.000000 |
| Carbon | <i>p</i> | 18.1557 | 0.039196 | Oxygen | <i>s</i> | 0.0073 | 1.000000 |
| Carbon | <i>p</i> | 3.98640 | 0.244144 | Oxygen | <i>p</i> | 0.0822 | 1.000000 |
| Carbon | <i>p</i> | 1.14290 | 0.816775 | Oxygen | <i>p</i> | 0.0316 | 1.000000 |
| Carbon | <i>p</i> | 0.35940 | <u>1.000000</u> | Oxygen | <i>p</i> | 0.0122 | 1.000000 |
| Carbon | <i>p</i> | 0.11460 | 1.000000 | Supplemental scattering basis, Π_g symmetry | | | |
| Carbon | <i>d</i> | 0.75000 | 1.000000 | Carbon | <i>d</i> | 1.5 | 1.000000 |
| Oxygen | <i>s</i> | 7816.54 | 0.006436 | Carbon | <i>d</i> | 0.3 | 1.000000 |
| Oxygen | <i>s</i> | 1175.82 | 0.048924 | Carbon | <i>d</i> | 0.15 | 1.000000 |
| Oxygen | <i>s</i> | 273.188 | 0.233819 | Oxygen | <i>p</i> | 0.0822 | 1.000000 |
| Oxygen | <i>s</i> | 81.1696 | 0.784798 | Oxygen | <i>p</i> | 0.0316 | 1.000000 |
| Oxygen | <i>s</i> | 27.1836 | <u>0.803381</u> | Oxygen | <i>d</i> | 0.4 | 1.000000 |
| Oxygen | <i>s</i> | 3.41360 | 0.316720 | Supplemental scattering basis, Δ_g symmetry | | | |
| Oxygen | <i>s</i> | 9.53220 | <u>1.000000</u> | Carbon | <i>d</i> | 1.5 | 1.000000 |
| Oxygen | <i>s</i> | 0.93980 | 1.000000 | Carbon | <i>d</i> | 0.375 | 1.000000 |
| Oxygen | <i>s</i> | 0.28460 | 1.000000 | Carbon | <i>d</i> | 0.18 | 1.000000 |
| Oxygen | <i>p</i> | 35.1832 | 0.040023 | Carbon | <i>d</i> | 0.10 | 1.000000 |
| Oxygen | <i>p</i> | 7.90400 | 0.253849 | Carbon | <i>d</i> | 0.05 | 1.000000 |
| Oxygen | <i>p</i> | 2.30510 | 0.806841 | Oxygen | <i>d</i> | 1.70 | 1.000000 |
| Oxygen | <i>p</i> | 0.71710 | <u>1.000000</u> | Oxygen | <i>d</i> | 0.40 | 1.000000 |
| Oxygen | <i>p</i> | 0.21370 | 1.000000 | Oxygen | <i>d</i> | 0.20 | 1.000000 |
| Oxygen | <i>d</i> | 0.85000 | 1.000000 | Oxygen | <i>d</i> | 0.10 | 1.000000 |

^aUnderlines separate contracted basis functions.

$D_{\infty h}$ in discussing our results, we note that the calculations were actually carried out in the reduced symmetry group D_{2h} , since our molecular structure codes are restricted to Abelian point groups.

A. Static exchange

The static-exchange (SE) approximation neglects all target relaxation effects: i.e., no $(N+1)$ -electron CSFs Θ_i are included in the trial wave function. This level of approximation is well known to be quantitatively, and often qualitatively, incorrect at scattering energies below several eV, but generally displays the basic features of the scattering at higher energies. Since the SE cross section is a well-defined quantity that should be independent of the method used to perform the calculation, we report results at this level in order to compare with previous *ab initio* calculations and to gauge the accuracy of our calculations with respect to choice of trial basis, number of continuum angular momenta included, and the numerical procedures employed.

B. Polarized SCF

To treat the scattering at low energies, it is important to describe the dynamic polarization of the target by the incident electron. Previous work on a variety of closed-shell targets has shown that including a particular set of configurations in Eq. (1) to produce what is known as a ‘‘polarized-SCF’’ (PSCF) trial function [12] provides a good description of target polarization, while maintaining a balance of correlation effects in the N - and $(N+1)$ -electron systems. The PSCF trial function includes $(N+1)$ -electron CSFs Θ_i constructed from the product of bound molecular orbitals and terms obtained by singly exciting the target SCF wave function. Thus the configurations Θ_i in Eq. (1) have the form

$$\Theta_i = A(\chi_0[\varphi_0 \rightarrow \varphi_\alpha]\varphi_i), \quad (8)$$

where $\varphi_0 \rightarrow \varphi_\alpha$ denotes the replacement of occupied orbital φ_0 by φ_α and φ_i is another virtual orbital. Instead of using all the occupied orbitals to define a space of singly excited CSFs, we choose a compact subspace of the virtual orbitals, the polarized virtual orbitals denoted as φ_α in Eq. (8), for

singly exciting the target. The polarized orbitals are defined in first-order perturbation theory as the adiabatic response of a target SCF orbital to an externally applied electric field. In general, there will be three polarized orbitals for every occupied SCF orbital, one for each Cartesian component of the dipole operator (μ_α). The polarized orbitals are obtained by diagonalizing the operator

$$P_{ij}^\alpha = \frac{\langle \varphi_i | \mu_\alpha | \varphi_0 \rangle \langle \varphi_0 | \mu_\alpha | \varphi_j \rangle}{(\varepsilon_i - \varepsilon_0)(\varepsilon_j - \varepsilon_0)} \quad (9)$$

in the space of ‘‘improved virtual orbitals’’ φ_i , which are eigenfunctions of a *singlet* V_{N-1} Fock operator obtained by removing one electron from the doubly occupied orbital φ_0 . It is important to bear in mind that these polarized orbitals are not intended to give an accurate description of individual excited target states, but rather a basis for describing the dynamic response on the target to an incident electron. Further details about the polarized-SCF model can be found elsewhere [12].

We generated a set of polarized orbitals from the six highest occupied orbitals. Single excitations from these occupied SCF orbitals into the polarized orbitals give a polarizability of 13.23 a.u., which is 84% of the experimentally determined value [13]. This indicates that using a SCF description of the target should be a reasonable approximation. Note that in constructing the polarized orbitals, the entire space of target and supplemental basis functions listed in Table I was used.

Polarized-SCF trial functions were constructed for the total symmetries ${}^2\Sigma_g^+$, ${}^2\Sigma_u^+$, and ${}^2\Pi_g$. The total number of L^2 configurations in these symmetries was 2085, 2081, and 840, respectively. The form of the Kohn trial function employed here [Eq. (1)] is only appropriate for electronically elastic scattering. With the polarized orbital basis we used, a single-excitation configuration-interaction calculation showed that the excitation energy of the lowest triplet state of the target was 8.7 eV. Although we might expect calculations carried out above this energy with a trial function of the type we used to show spurious resonances due to neglect of energetically open channels, they are evidently quite narrow and are not apparent in our calculations, which extend up to 10 eV.

C. Relaxed SCF

In symmetries that include shape resonances, the polarized-SCF model may not give the best description of the quasibound negative ion. The dominant effect included in the polarized-SCF model is the dynamic polarization of the target orbitals through single excitations into a set of unoccupied orbitals that are optimized to reproduce the target polarizability. In the polarized-SCF model, we include excitations from a given occupied orbital into all polarized orbitals, irrespective of symmetry, and we include both singlet and triplet intermediate spin couplings. While this prescription generally gives a good description of target polarization, it may lead to an unbalanced description of correlation in the temporary negative-ion state relative to the SCF target state at short range, with the result that the resonance will appear at too low an energy relative to the target ground state. This

turned out to be true in the present case, with the PSCF treatment placing the ${}^2\Pi_u$ resonance at 3 eV, which is approximately 1 eV too low.

For a number of closed-shell target molecules, we have found that a relaxed-SCF trial wave function gives a more balanced description of low-energy shape resonances. The relaxed-SCF trial function only includes configurations Θ_i in Eq. (1) built from *singlet-coupled*, single excitations of the occupied target orbitals into virtual orbitals of the same symmetry. We do not include any configurations that break the spatial or spin symmetry of the ground state. This type of trial function describes the essential short-range core relaxation effects that would be present in a SCF calculation on the negative ion, but does not include the spin- and dipole-polarization effects of the polarized-SCF model. Such a treatment has been shown to give a good description of shape resonances in electron- N_2 [14], H_2CO [15], C_2H_4 [16], N_2O [17], and BCl_3 [18]. This treatment was used for the ${}^2\Pi_u$ symmetry component of the scattering in the resonance region. For this case, the number of L^2 terms in the trial wave function was 840. Note that there is no problem with ground-state recorelation in either the polarized-SCF or relaxed-SCF treatments, since Brillouin’s theorem guarantees that single excitations cannot change a closed-shell SCF target state.

D. Approximate treatment of nuclear motion

Most previous theoretical treatments of $e\text{-CO}_2$ scattering have been carried out with the nuclei fixed at their equilibrium positions. (Significant exceptions include an early study by Morrison and Lane [19] of the threshold energy behavior of the symmetric-stretch mode and the recent work of Morgan [4] on the behavior of the CO_2^- virtual state under bending.) To our knowledge, there have been no previous *ab initio* studies of the effect of vibrational motion on cross section in the vicinity of the 3.8 eV resonance.

Cadez *et al.* [20] have noted that resonant vibrational excitation of CO_2 couples most strongly to the symmetric-stretch mode, having observed energy-loss spectra at 4 eV for pure symmetric-stretch vibration up to $v' = 25$. We have therefore undertaken a preliminary study of the importance of nuclear motion on the computed integral and differential cross sections, using the adiabatic nuclei treatment outlined in Sec. III and considering only the effect of symmetric-stretch motion on the resonant ${}^2\Pi_u$ components of the scattering amplitude.

Symmetric-stretch motion does not break the Σ_g^+ symmetry of the target, so we can continue to use the $D_{\infty h}$ symmetry designations. Focusing on the ${}^2\Pi_u$ ($|m|=1$, l odd) component of the T matrix, we first separate it into resonant and nonresonant components. This is most easily accomplished by working in the eigenphase representation [21], viz.,

$$T_{ll'}^{\pi u} = \sum_\lambda c_l^\lambda c_{l'}^\lambda e^{i\delta_\lambda^{\pi u}} \sin(\delta_\lambda^{\pi u}). \quad (10)$$

The mixing coefficients c_l^λ are elements of the unitary matrix of eigenchannel vectors that diagonalize the T matrix and $\delta_\lambda^{\pi u}$ are the eigenphases. Figure 1 shows the energy depen-

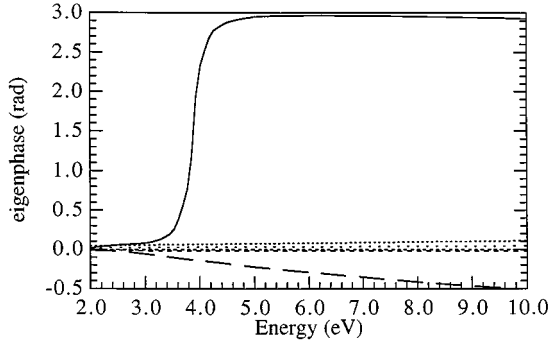


FIG. 1. Energy dependence of the fixed-nuclei ${}^2\Pi_u$ eigenphases for e -CO₂ scattering calculated at the equilibrium geometry.

dence of the ${}^2\Pi_u$ eigenphases calculated at the equilibrium position. The resonance behavior is clearly concentrated in one eigenphase $\delta_{\lambda_{\text{res}}}^{\pi_u}$, while the other eigenphases are small and smoothly varying. Similar behavior was found when the CO bond distance was varied, with the resonance eigenphase varying rapidly with CO distance, while the other eigenphases showed little dependence on geometry. Thus we could separate out the resonant term from the sum in Eq. (10) and ignore the geometry dependence of the nonresonant contributions. We carried out fixed-nuclei calculations at five linear geometries, corresponding to CO bond distances of $R = 2.0892, 2.1444, 2.1944, 2.2443, \text{ and } 2.2996$ a.u. At each geometry, the resonant eigenphase was fit to a Breit-Wigner form

$$[\sin \delta_{\lambda_{\text{res}}}(R)]^2 = \frac{[\Gamma(R)/2]^2}{[E - E_{\text{res}}(R)]^2 + [\Gamma(R)/2]^2}. \quad (11)$$

The mixing coefficients $c_l^{\lambda_{\text{res}}}(R)$, as well as the derived values of Γ and E_{res} , were all found to vary smoothly with R and could easily be interpolated to give the resonant T -matrix elements at any value of R . To complete the treatment, we approximated the symmetric-stretch vibrational wave functions of CO₂ by harmonic oscillator functions, using force constants derived from experimental data, and carried out the appropriate one-dimensional integrals over the symmetric stretch normal mode coordinate.

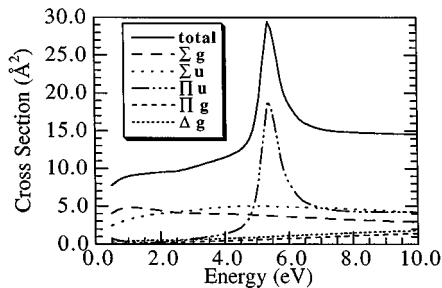


FIG. 2. Fixed nuclei, e -CO₂ total cross sections at the static-exchange level. Figure shows the total cross section as well as individual symmetry components.

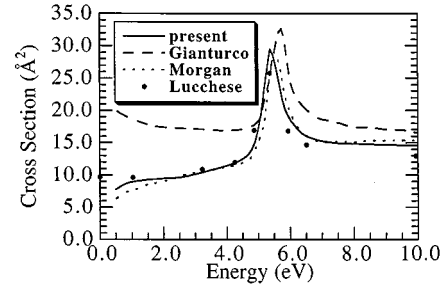


FIG. 3. Fixed nuclei, e -CO₂ total cross sections at the static-exchange level. Comparison of present results with previous *ab initio* work: Lucchese and McKoy [3], Morgan [4], and Gianturco and Stoecklin [22].

V. RESULTS

In Figs. 2 and 3, we show static-exchange cross sections computed at the equilibrium geometry. Our total integrated cross sections are shown in Fig. 2, along with the individual symmetry components. We see that the static-exchange approximation places the ${}^2\Pi_u$ near 6 eV, some 2 eV higher than experiment, and gives a total cross section that is relatively flat on the low-energy side of the resonance, with no sign of any enhancement below 2 eV. For comparison, we compare our total cross section with the results of other [3,4,22] theoretical static-exchange calculations in Fig. 3. All the results shown included a proper treatment of the nonlocal electron-exchange interactions and differ only in the numerical methods employed. In general, there is excellent agreement between the results at this level, except for the calculations of Gianturco and Stoecklin [22] which place the resonance slightly higher in energy and show a rising total cross section at low energies not evident in the other theoretical calculations at the static-exchange level.

In Fig. 4, we show the total cross sections we obtained at the equilibrium geometry when electron-target correlation is included. For the ${}^2\Sigma_g$, ${}^2\Sigma_u$, and ${}^2\Pi_g$ symmetries, the calculations were performed using a polarized-SCF trial function. For the ${}^2\Pi_u$ case, we used a PSCF trial function only for scattering energies below 2.0 eV, while for energies >2.0 eV we used the relaxed-SCF treatment outlined in Sec. IV C. The ${}^2\Delta_g$ symmetry component is unimportant at low energy

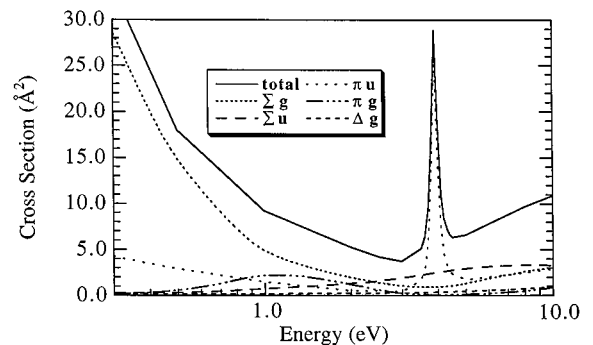


FIG. 4. Fixed nuclei, e -CO₂ total cross sections including electron-target correlation. See text for description of trial wave functions employed.

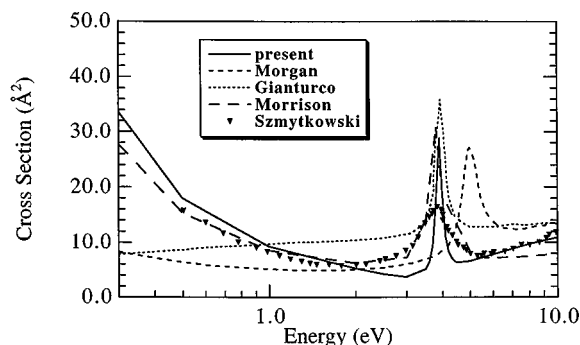


FIG. 5. Fixed nuclei, e -CO₂ total cross sections including electron-target correlation. Comparison of present results with previous theory: Morrison *et al.* [1], Morgan [4], and Gianturco and Stoecklin [22]. Experimental results are those of Szmytkowski *et al.* [25].

and was only treated at the static-exchange level. Several features about these cross sections are worth noting. The inclusion of target polarization has the expected effect on the $^2\Sigma_g^+$ component of the cross section at low energies, with the virtual state enhancement of the cross section below 2 eV clearly evident.

A virtual state is not a physical state, in the sense of a true bound state or even an autoionizing state. Mathematically, it corresponds to a pole of the S matrix on the negative imaginary momentum axis close to the origin. If this pole were to move onto the positive imaginary momentum axis under some change in the nuclear geometry away from equilibrium, it would be a bound state of the negative ion. To verify that our polarized-SCF treatment did not produce a bound state of CO₂⁻ in $^2\Sigma_g^+$ symmetry, we diagonalized the negative-ion Hamiltonian in the space of the 2085 L^2 configurations used to construct the trial wave function. The lowest eigenvalue obtained was indeed 0.12 eV *higher* than the target SCF energy of CO₂. This result is also consistent with the *ab initio* study of Morgan [4], who found a CO₂⁻ virtual state in linear geometry that became weakly bound when the O-C-O angle was bent to $\sim 145^\circ$. It is also worth noting that there have been several bound-state studies [23,24] on CO₂ and CO₂⁻ which show that the negative ion is electronically bound at bent geometries. However, this ground state of bent CO₂⁻ correlates with the 3.8 eV $^2\Pi_u$ resonance state in linear geometry [24], *not* the $^2\Sigma_g^+$ virtual state. It is probably the case that the virtual state, upon bending, becomes a diffuse, weakly bound, dipole state, but clearly this will require further study.

The relaxed-SCF treatment of the $^2\Pi_u$ component of the cross section places the resonance peak near 3.8 eV, in good agreement with experiment, and gives a broad secondary peak at very low energies. This behavior is consistent with that found by Gianturco and Stoecklin [22] in their static-exchange-polarization calculations. The effect of inclusion of polarization in $^2\Sigma_u^+$ symmetry is to reduce the cross section substantially relative to the static-exchange result, while the $^2\Pi_g$ and $^2\Delta_g$ components remain relatively unimportant below 10 eV.

Figure 5 compares our total, fixed-geometry results with the recent R -matrix calculations of Morgan [4], as well as the

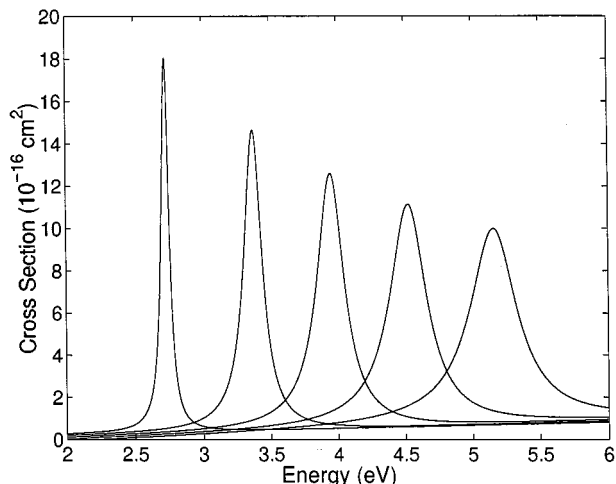


FIG. 6. Symmetric-stretch dependence of the fixed-nuclei, $^2\Pi_u$ component of the integrated cross section. The five curves shown are for CO bond distances of 2.0892, 2.1444, 2.1944, 2.2443, and 2.2996 a.u. The resonance energy is lowered as the CO distance is increased.

static-exchange-polarization results of Gianturco and Stoecklin [22] and Morrison, Lane, and Collins [1]. The experimental total scattering cross section measurements are those of Szmytkowski *et al.* [25]. The fixed-nuclei results calculated at the equilibrium geometry give a resonance peak which is substantially higher and narrower than experiment. This is the behavior that prompted us to consider the effects of nuclear motion on the resonance symmetry.

Figure 6 shows the fixed-nuclei integrated $^2\Pi_u$ cross sections at five different values of the CO bond distance. It is clear that the resonance is very sensitive to changes in the CO bond distance, becoming narrower and lower in energy as the molecule is stretched. Incorporating this dependence on CO symmetric stretch into our calculations via the treatment outlined in Sec. IV D gives the results shown in Fig. 7. This figure shows the integrated total and vibrationally elastic cross sections, both experimental and calculated. The effect of nuclear motion is clearly to broaden and lower the

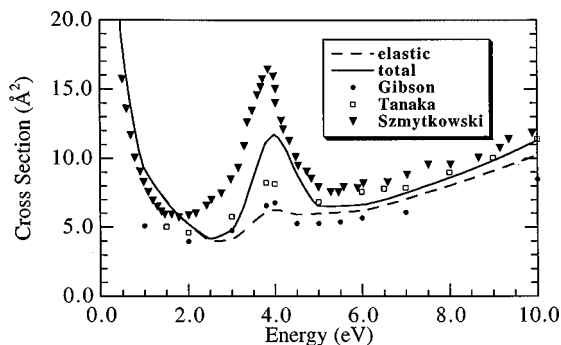


FIG. 7. Total and vibrationally elastic e -CO₂ integrated cross sections incorporating an adiabatic-nuclei treatment of symmetric-stretch motion. Experimental results are those of Szmytkowski *et al.* [25] for the total cross section and Tanaka *et al.* [5] and Gibson *et al.* [6] for the elastic cross sections.

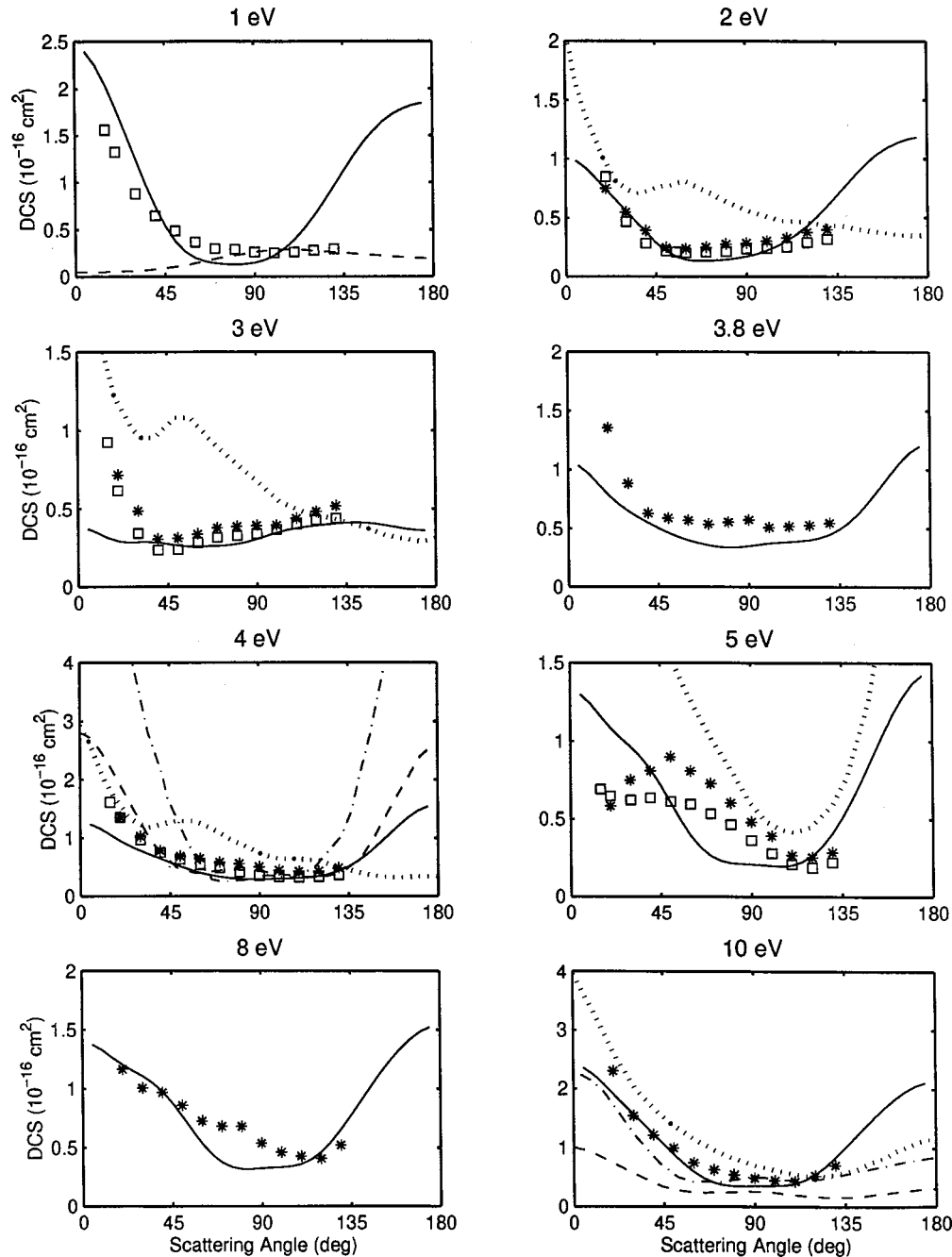


FIG. 8. Elastic differential cross sections for e -CO₂ scattering. Present results incorporate an adiabatic-nuclei treatment of symmetric-stretch motion. Solid curves: present results. Dotted curves: Tanaka *et al.* [5]. Dashed curves: Gianturco and Stoecklin [22]. Dot-dashed curves: Morrison *et al.* [1]. Experimental results are those of Tanaka *et al.* [5] (open squares) and Gibson *et al.* [6] (asterisks).

resonance feature, bringing our calculated cross sections into better agreement with experiment. The elastic cross sections are of course smaller than the total cross sections, particularly in the region of the shape resonance, indicating that a substantial fraction of the total cross section corresponds to vibrational excitation. Note that at energies below 2 eV and above 5 eV, outside the resonance region, our total and integral elastic cross sections are approximately equal. This is to be expected since our approximate treatment of vibrational motion was restricted to the resonant portion of the $^2\Pi_u$ scattering.

Our vibrationally elastic cross sections are in much better agreement with experiment than our results for the total cross

section. This difference in agreement is to be expected, since the elastic scattering amplitudes only sample the geometry dependence of the fixed-nuclei T -matrix elements in a restricted region about their equilibrium values. Additional approximations are needed to arrive at the adiabatic-nuclei expression for the total (vibrationally summed) cross section [Eq. (7)], namely, the use of a closure approximation which ignores the dependence of the T -matrix elements on vibrational energy differences. A more sophisticated treatment of nuclear motion is needed to quantitatively describe the vibrationally summed cross section.

In Fig. 8, we plot our elastic differential cross sections along with the recent measurements of Tanaka *et al.* [5] and

Gibson *et al.* [6], as well as previous theoretical results. At 1.0 and 2.0 eV, the present results show quantitative agreement with the measured values. At the resonance energy (3.8 eV), the DCS shows near symmetry about 90°, confirming that a single resonance symmetry dominates the scattering [26]. At energies just below the resonance, we see the largest disagreement: at 3.0 eV the calculations fail to show the strong forward peak found in the experiments. We suspect that in this transitional region just below the resonance, vibrational effects, along with mixed resonant and direct scattering, combine more subtly than our simplified single-mode model of nuclear motion can describe. At the higher scattering energies, polarization effects lose their importance and most approaches do a reasonable job of reproducing the measured data. Overall, we find good agreement with the mutually consistent sets of data from Refs. [5] and [6].

VI. DISCUSSION

We have presented the first *ab initio* electron-CO₂ scattering calculations that quantitatively reproduce the two main low-energy features of the system: the strong rise of the cross section near zero energy associated with the virtual state and the temporary negative-ion resonance at 3.8 eV. A proper treatment of electron correlation effects is essential in

both cases; we have used a polarized-SCF approach for all symmetries except the $^2\Pi_u$ component above 2.0 eV, for which a relaxed-SCF method is more appropriate.

While the fixed-nuclei calculations at equilibrium geometry place the resonance at the experimentally observed energy, we found the fixed-nuclei resonance to be too narrow. We also found that a simple adiabatic treatment of the symmetric-stretch vibrational mode largely repairs this deficiency.

There remain some details, especially in several of the low-energy differential cross sections and in the shape of the total cross section in the low-energy wing of resonance, for which the present approach appears insufficient. In future work, we intend to explore the effects of all target vibrational modes on *e*-CO₂ scattering.

ACKNOWLEDGMENTS

This work was performed under the auspices of the U.S. Department of Energy by the Lawrence Livermore National Laboratory and the Lawrence Berkeley National Laboratory under Contract Nos. W-7405-Eng-48 and DE-AC03-76SF00098, respectively. The authors wish to acknowledge the use of computational resources of the National Energy Research Scientific Computing Center.

-
- [1] M. A. Morrison, N. F. Lane, and L. A. Collins, *Phys. Rev. A* **15**, 2186 (1977).
- [2] M. A. Morrison, *Phys. Rev. A* **25**, 1445 (1982).
- [3] R. R. Lucchese and V. McKoy, *Phys. Rev. A* **25**, 1963 (1982).
- [4] L. A. Morgan, *Phys. Rev. Lett.* **80**, 1873 (1998).
- [5] H. Tanaka, T. Ishikawa, T. Masai, T. Sagara, L. Boesten, M. Takekawa, Y. Itikawa, and M. Kimura, *Phys. Rev. A* **57**, 1798 (1998).
- [6] J. C. Gibson, M. A. Green, K. W. Trantham, P. J. O. Teubner, and M. J. Brunger, *J. Phys. B* **32**, 213 (1999).
- [7] T. N. Rescigno, B. H. Lengsfeld III, and C. W. McCurdy, in *Modern Electronic Structure Theory*, edited by D. R. Yarkony (World Scientific, Singapore, 1995), p. 501.
- [8] T. N. Rescigno, C. W. McCurdy, A. E. Orel, and B. H. Lengsfeld III, in *Computational Methods for Electron-Molecule Collisions*, edited by W. M. Huo and F. A. Gianturco (Plenum, New York, 1995), p. 1.
- [9] N. F. Lane, *Rev. Mod. Phys.* **52**, 29 (1980).
- [10] D. M. Chase, *Phys. Rev.* **104**, 838 (1956).
- [11] T. H. Dunning, *J. Chem. Phys.* **53**, 2823 (1970).
- [12] B. H. Lengsfeld III, T. N. Rescigno, and C. W. McCurdy, *Phys. Rev. A* **44**, 4296 (1991).
- [13] M. A. Morrison and P. J. Hay, *Phys. Rev. A* **20**, 740 (1979).
- [14] A. U. Hazi, T. N. Rescigno, and M. Kurilla, *Phys. Rev. A* **23**, 1089 (1981).
- [15] T. N. Rescigno, C. W. McCurdy, and B. I. Schneider, *Phys. Rev. Lett.* **63**, 248 (1989).
- [16] B. I. Schneider, T. N. Rescigno, B. H. Lengsfeld III, and C. W. McCurdy, *Phys. Rev. Lett.* **66**, 2728 (1991).
- [17] C. Winstead and V. McKoy, *Phys. Rev. A* **57**, 3589 (1998).
- [18] W. A. Isaacs, C. W. McCurdy, and T. N. Rescigno, *Phys. Rev. A* **58**, 2881 (1998).
- [19] M. A. Morrison and N. F. Lane, *Chem. Phys. Lett.* **66**, 527 (1979).
- [20] I. Cadez, F. Greteau, M. Tronc, and R. I. Hall, *J. Phys. B* **10**, 3821 (1977).
- [21] See, for example, R. K. Nesbet, *Variational Methods in Electron-Atom Scattering Theory I* (Plenum, New York, 1980).
- [22] F. A. Gianturco and T. Stoecklin, *J. Phys. B* **29**, 3933 (1996).
- [23] J. Pacansky, U. Wahlgren, and P. S. Bagus, *J. Chem. Phys.* **62**, 2740 (1975).
- [24] Y. Yoshioka and H. F. Schaefer III, *J. Chem. Phys.* **75**, 1040 (1981).
- [25] C. Szmytkowski, A. Zecca, G. Karwasz, S. Oss, K. Maciag, B. Mannkovic, R. S. Brusa, and R. Grisenti, *J. Phys. B* **20**, 5817 (1987).
- [26] D. Andric and F. H. Read, *J. Phys. B* **4**, 389 (1971).